JOURNAL OF MATERIALS SCIENCE 31 (1996) 485–490

An X-ray absorption study of doped silicate glass, fibre optic preforms

D. T. BOWRON, R. J. NEWPORT, J. S. RIGDEN
The Physics Laboratory, The University of Kent at Canterbury, Canterbury, Kent, CT2 7NR, UK

E. J. TARBOX
Optical Systems Group, Pirelli Cables Ltd, Leigh Road, Eastleigh, Hants, S05 5YE, UK

M. OVERSLUIZEN
Daresbury Laboratory, Warrington, Cheshire, WA4 4AD, UK*

Optical fibre preforms, which have their germanosilicate core regions doped with small quantities of the rare-earth element erbium, have been studied using Extended X-ray Absorption Fine Structure Spectroscopy (EXAFS) at the germanium K absorption edge. These studies were performed using a circular X-ray beam of 100 μm diameter, allowing information to be gathered as a radial function of position across the core region of the preform. This positioning was accomplished by means of a motorized pinhole collimator and sample stage developed for use on the focused X-ray beamline 8.1, at the SRS, Daresbury Laboratory, UK. The EXAFS results are consistent with the germanium sites coordinated to surrounding oxygen atoms at a mean distance of 0.17 nm. Absorption maps of the rare-earth and germanium distribution across the core region of the preforms have also been obtained, showing a correlation between the distributions of the two atom types.

1. Introduction

Optical fibre preforms are the penultimate step in the production of optical fibre, for use in the telecommunications, sensor and opto-electronics industries. They possess all the properties of the final fibre, except on a larger scale; typical experimental preforms have an external diameter of approximately 15 mm and a core diameter of approximately 1 mm, and would be sleeved and drawn into, for example, a single mode fibre with a core diameter of 4 μm. Rare-earth doped silicate fibres are of particular importance in the construction of optical devices, such as fibre amplifiers and lasers. The samples studied here were manufactured using modified chemical vapour deposition (MCVD) [1], and solution doped with erbium ions [2]. The germanium codopant was introduced as a vapour in the initial deposition process.

The manufacturing technique leads to cylindrical symmetry of the deposited system, although radial variations in dopant atom concentration are evident; poorly formed preforms may display non-cylindrical symmetry in the structure of the core. The rare-earth dopant is incorporated into the preforms as the active optical element, and the germanium codopant is included to increase the refractive index of the preform core.

The rare-earth dopant is present in concentrations less than 1 wt %, making (EXAFS) experiments extremely difficult to perform, a problem which is compounded by the small sample volumes available for structural study. Attempts at obtaining EXAFS spectra at the Er L_{III} edge (8364 eV) have been made, pushing current synchrotron facilities to their utmost limits, and reliable data have proved difficult. Fluorescence spectra have been obtained from the entire core of a neodymium doped sample [3], a system with possible sensor applications; but this preform core has a rare-earth concentration of approximately 4 wt % and spatially resolved studies of structure as a function of radial position were not made.

The EXAFS experiments at the Ge K edge (11 105 eV) were easier to perform, the codopant being present in quantities ranging between 15 and 18 wt %. The spectra were obtained in a conventional transmission mode. The need for high spatial resolution necessitates the use of small incident beam sizes resulting in low photon flux at the sample; thin samples are therefore required to avoid excessive attenuation of the transmitted beam.

2. Experimental procedure

The experiments were performed on station 8.1 at the SRS, Daresbury Laboratory, UK. The storage ring parameters being at an electron energy of 2 GeV and with a ring current of between 200 and 300 mA; the

*Affiliated with the Nederlandse Organisatie voor Wetenschappelijk Onderzoek (NWO).

0022–2461

beam current half-life was on average 30 h and a daily refill procedure was in practice. The station uses a Pt-coated quartz torroidal 3:1 focusing mirror, providing a flux of $4–6 \times 10^{11}$ photons s^{-1} in a beam spot of approximate dimensions 3×1.2 mm^2 [4]. The focusing optics are of vital importance if a useful flux is to be obtained with the 100 μm pinhole collimation system. This station is equipped with a double bent, water cooled, order-sorting, slitless Si(2 2 0) monochromator crystal, which gives access to a photon energy range between 5.2 and 11.5 keV. This energy range unfortunately limits the accessible data range beyond the germanium K edge.

The experimental geometry for the measurements was that for standard transmission EXAFS, with the addition of a motorized pinhole collimator stage and sample stage to allow controlled positioning of the sample from a remote terminal; a schematic diagram is shown in Fig. 1. These stages allow for the repeatable positioning of the sample and pinhole to an accuracy of 0.01 mm in both the vertical and horizontal planes. The collimator stage has two additional degrees of motional freedom, providing yaw and pitch adjustments. Together these allow the transmitted flux to be maximized.

The samples were transverse slices of fibre preform initially 1–2 mm thick, then ground to a thickness of approximately 100 μm by a lapping and polishing process. This thinning was performed on a rotary polishing bed using 3 μm aluminium oxide powder as the crude lapping agent and 0.5 μm cerium oxide polishing powder for the final stages of thinning, prior to mounting the sample upon aluminium frames, see Fig. 1.

The distribution of the dopant atoms was probed by a tracking procedure, where the core was stepped across the 100 μm beam, while the absorption of the sample was monitored. The wavelength of the incident beam is chosen to be just above the relevant absorption edge energy for the atom type whose concentration is being mapped. This produces an absorption profile, averaged across the 100 μm beam diameter, illuminating the sample. An iterative procedure was adopted to obtain an absorption profile across two perpendicular diameters of the sample core region. The results of this mapping are shown in Figs 2–7.

Once the collimator and sample had been aligned, experiments could proceed until the next daily storage

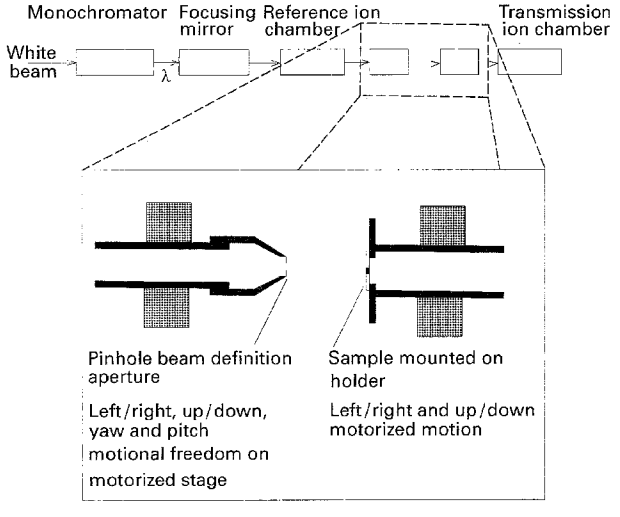

Figure 1 Schematic diagram: station 8.1, SRS, Daresbury Laboratory.

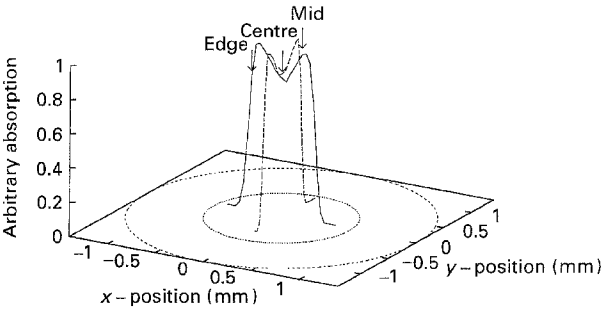

Figure 2 Sample A: fibre preform core absorption profile, Ge edge.

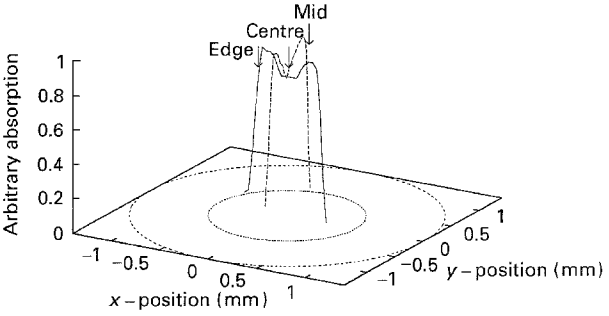

Figure 3 Sample A: fibre preform core absorption profile, Er edge.

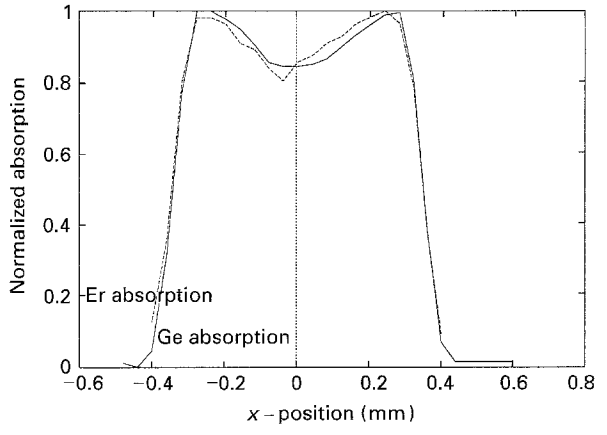

Figure 4 Absorption profiles, sample A.

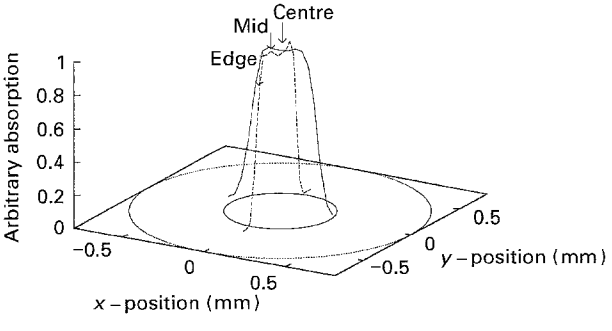

Figure 5 Sample B: fibre preform core absorption profile, Ge edge.

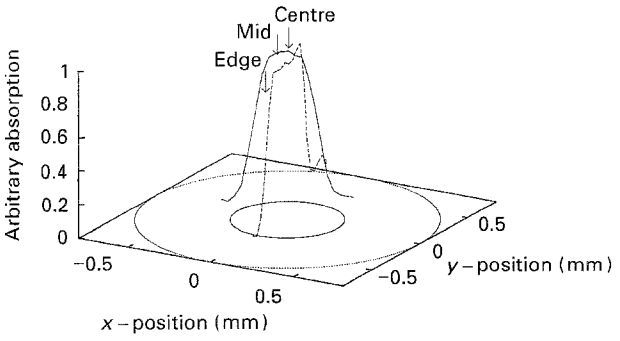

Figure 6 Sample B: fibre preform core absorption profile, Er edge.

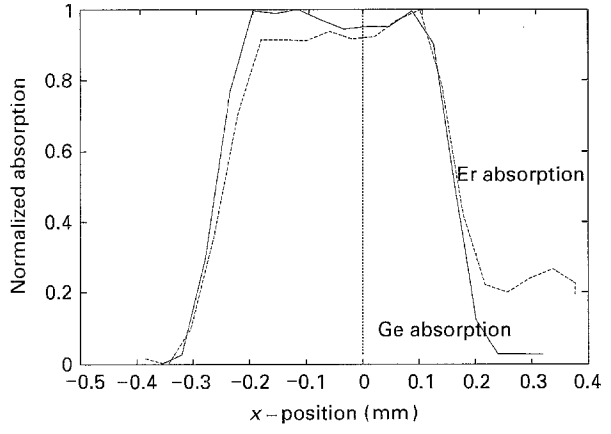

Figure 7 Absorption profiles, Sample B.

ring refill, after which the beam position was found to move slightly, requiring the repositioning of the pinhole and sample, and hence remapping of the core before experiments could continue.

3. Theory

The EXAFS data analysis was performed using the standard Daresbury Laboratory EXAFS analysis suite of programs, namely EXCALIB, EXBACK and EXCURV90 [5], which, respectively, perform the tasks of

1. summation of multiple data sets and calibration of their edges and absorptions,
2. background subtraction and normalization of the EXAFS signal, and
3. fitting of the EXAFS spectrum by means of the fast curved wave theory [6, 7].

Examination of the phenomenological plane wave equation, which can be used to describe the EXAFS spectra, shows the relationships between parameters, i.e.

$$\chi(\boldsymbol{k}) = A(\boldsymbol{k})\sum_i \frac{N_i}{\boldsymbol{k}R_i^2}|f(\boldsymbol{k}, \pi)_i|\sin(2\boldsymbol{k}R_i + 2\delta + \varphi_i)$$

$$\exp\left(\frac{-2R_i}{\lambda}\right)\exp(-2\sigma_i^2\boldsymbol{k}^2) \quad (1)$$

Since no suitable standards, i.e. analogous Ge–Er glass compounds with known structure, were available, calibration of the sample dependent parameters in the EXAFS model [notably the amplitude reduction factor $A(k)$ accounting for inelastic scattering effects damping the EXAFS signal] was not possible. This increases the level of uncertainty associated with the evaluated co-ordination numbers, N_i; the quoted error bars attempt to include the effects.

In EXAFS, $\boldsymbol{k}$ is the wave vector of the freed photoelectron. Note the direct correlation in the two variables $A(\boldsymbol{k})$ and N_i. $A(\boldsymbol{k})$ typically varies between 0.7 and 0.9, dependent upon the atomic number of the excited atom type; if no calibrant system is available this will increase the apparent variation in N_i. The other parameters in this expression are R_i, the distance between the excited atom and the neighbouring ith backscattering atom; $f(\boldsymbol{k}, \pi)_i$, a measure of the strength of backscattering of the atom type i; δ_i, the phase shift induced in the electron wave as it propagates through the excited atom potential, and φ, the phase shift induced by the backscattering atom potential; λ, a mean free path term to account for the finite lifetime of the propagating electron wave; and σ, the exponent in the Debye–Waller term to account for static and vibrational disorder in the structural system under examination.

The plane wave equation is a useful heuristic model for EXAFS, but is not used in the EXCURV90 [5] code; this uses either the far more reliable fast curved wave theory [6, 7] or the small atom approximation [8].

4. Results and discussion

The results of the absorption profile mapping, as shown in Figs 2–7, graphically demonstrate the correlation between the concentration profiles of the two dopant atom species, erbium and germanium; the plots have been normalized such that the maximum absorption measured during a scan at a particular absorption edge is assigned a value of unity. The correlation between the concentration profiles is perhaps most clearly seen in the dip in the absorption profile at the central core region of sample A. The reduction in germanium concentration is expected in some cases due to evaporative loss of GeO_2. This loss occurs on sintering the deposited doped soot within the silica tube to form the glass that will ultimately be the preform–fibre core and also during the collapse phase. The depleted region is also visible in the erbium profile for sample A, indicating that the volatilization loss of GeO_2 also reduces the erbium concentration. Sample B does not show a dip in the central core region, a fact mirrored in the Er profile for this sample. This more uniform profile was achieved by the removal of the dopant loss region by means of an etch process implemented prior to collapsing the silica tube to form the preform. In both samples, the erbium concentration profile closely tracks that of the germanium, suggesting a measure of association between the sites occupied by the dopant species. This point is interesting, since the erbium is incorporated into the preform by means of solution doping [2], whereas germanium doping is achieved by the introduction of germanium containing vapour into the MCVD silica

tube as the core layers of SiO_2 soot are deposited. This would suggest that as the solution containing erbium ions is absorbed uniformly into the silica soot, it follows the germanium profile closely. A secondary ion mass spectrometry (SIMS) study of the distribution of dopant atomic species across preform and fibre cores has been performed on Er/Al and Er/Al/P doped silicate glass preforms and fibres [9], the study showing a dip in the phosphorus profile as the preform was mapped, but there was no corresponding dip in either the erbium or aluminium profiles. This implies that erbium is more closely associated with a germanium codopant than a phosphorus dopant, or that Er is bound closely with Al; Al_2O_3 does not volatilize during sintering or collapse phases.

EXAFS spectra were collected at the Ge K edge. As previously mentioned, only a limited k-range was accessible (to ~ 90 or $\sim 180\,nm^{-1}$ using convectional neutron–X-ray diffraction definitions), making data analysis slightly more problematic than usual. Phase shifts were determined theoretically, and the sample-dependent parameters, such as the reduction factor $A(k)$, and the mean free path term, λ, were fixed at nominal glass values and held constant between the spectra obtained at different core positions and between the different samples. This ensures consistency between results, and the quoted errors take these uncertainties into account.

The main problem of the limited k-range is the uncertainty introduced when determining the back-scattering atomic species. The first atom shell about the excited germanium central atom was, however, certainly oxygen, with fit parameters that suggest a pseudo body centred cubic arrangement of eight oxygen atoms about a central germanium atom. This result is considered anomalous as germanium in an oxide environment takes on a tetrahedral network structure of four oxygen atoms about each germanium atom, thus the value obtained of eight oxygens as the first shell coordination of the germanium atoms is almost twice what would have been expected. A possible explanation for this result is that due to the experimental geometry, i.e. the placement of the reference ion chamber prior to the pin-hole used to define the beam; any variation in beam intensity caused by drift of the beam upon the monochromator crystals

TABLE I Summary of EXAFS results (Ge K-edge)

Sample and position	Shell 1 (O)			Shell 2(Si)		
	Distance (nm ± 0.005)	CN (Atoms ± 1)	σ^2 (nm^2 ± 0.000 001)	Distance (nm ± 0.0005)	CN (Atoms ± 2)	σ^2 (nm^2 ± 0.000 004)
Sample A Centre	0.170	8.54	0.000 08	0.306	9.10	0.000 23
Mid	0.171	7.49	0.000 05	0.305	10.92	0.000 26
Edge	0.170	7.44	0.000 04	0.303	11.90	0.000 29
Sample B Centre	0.171	9.40	0.000 10	0.306	6.83	0.000 23
Mid	0.171	8.34	0.000 08	0.306	10.45	0.000 29
Edge	0.172	7.86	0.000 06	0.306	6.43	0.000 17

TABLE II Summary of EXAFS results (Ge K-edge)

Sample and position	Shell 1 (O)			Shell 2(Er)		
	Distance (nm ± 0.005)	CN (Atoms ± 1)	σ^2 (nm ± 0.000 001)	Distance (nm ± 0.005)	CN (Atoms ± 2)	σ^2 (nm ± 0.000 004)
Sample A Centre	0.170	8.54	0.000 05	0.300	15.99	0.000 29
Mid	0.171	7.66	0.000 05	0.300	13.66	0.000 29
Edge	0.170	6.93	0.000 03	0.298	21.86	0.000 40
Sample B Centre	0.171	9.33	0.000 10	0.300	14.32	0.000 32
Mid	0.171	8.34	0.000 08	0.299	19.60	0.000 40
Edge	0.172	8.01	0.000 06	0.300	9.97	0.000 23

resulting in a variation in X-ray intensity through the pin-hole would be uncorrected for in the analysis. Unfortunately, at the time of the experiment this problem was not considered; if future work of this kind is to be undertaken, arrangements would have to be made for the placement of some kind of intensity-monitoring device prior to the sample but post pin-hole, unless an exceptionally stable beam could be guaranteed from the source/monochromator arrangement. The second atomic shell data proves to be more difficult to interpret, although its presence is statistically

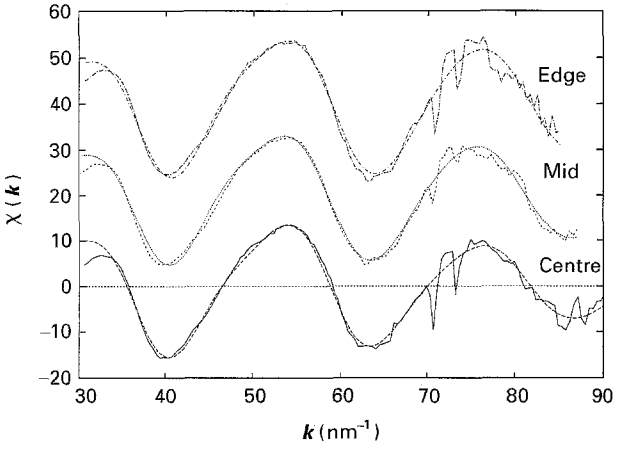

Figure 8 EXAFS spectra and theoretical fits for sample A, Ge edge.

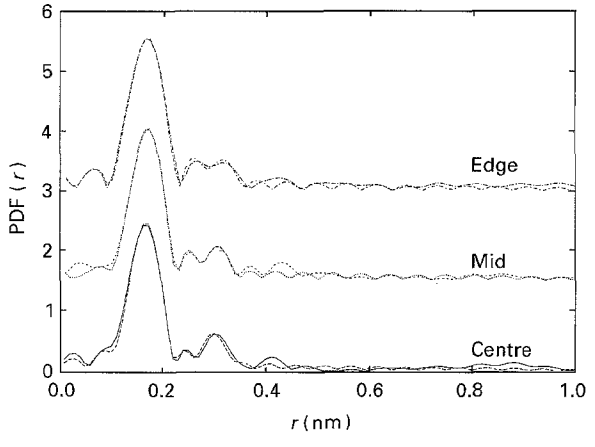

Figure 9 EXAFS PDFs and theoretical fits for sample A, Ge edge.

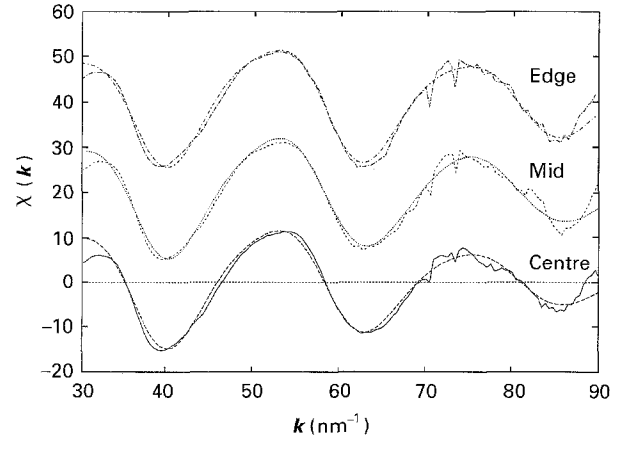

Figure 10 EXAFS spectra and theoretical fits for sample B, Ge edge.

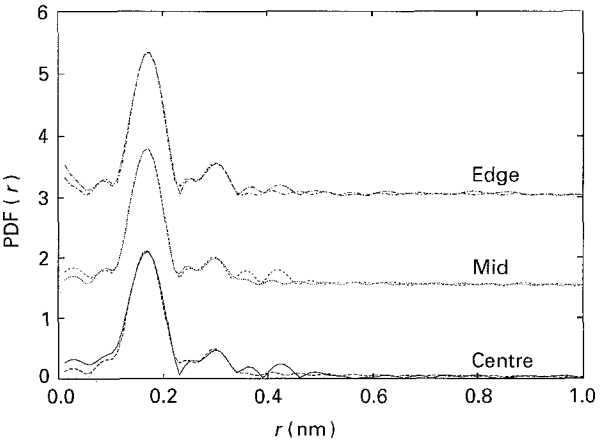

Figure 11 EXAFS PDFs and theoretical fits for sample B Ge edge.

significant [10]; the atomic species which can be used to fit the spectra for this shell could either be silicon, Table I, or erbium, Table II. The erbium gives a slightly better fit, but silicon is structurally the more likely major component to the shell, due to its dominance in the overall glass structure. The second shell may, however, contain some contributions from both atomic species, a hypothesis that unfortunately cannot be tested due to the limited k-range, and therefore low r-space resolution of the data. The magnitude of the Debye–Waller exponent, σ, indicates that the second shell contains a large distribution of distances, which would be consistent with this suggestion.

Fig. 8–11 show the spectra, and their respective Fourier transforms, obtained at each core position on the samples A and B. The theoretical fits to these spectra and transforms are also shown, as calculated for the parameters in Table I.

EXAFS spectra were attempted at the Er L_{III} edge, but, as anticipated, the signal proved to be too weak for viable analysis due to the extremely low concentrations of erbium present in the samples. EXAFS measurements in a fluorescence geometry would be far more favourable in this compositional range, but the small solid angle subtended by the fluorescence detector made this approach unfeasible. The local environment of erbium atoms in a bulk silicate glass matrix has been probed by EXAFS [11], results showing that the rare-earth takes up a local atomic arrangement similar to the environment that would be prevalent in Er_2O_3, i.e. six oxygen atoms surrounding each Er ion at a distance of 0.228 nm. In Er_2O_3 itself, there are six oxygens to each erbium, three at 0.2229 nm and three at 0.2317 nm [11]. The spectra obtained from the core region of sample A in a preliminary test at the erbium absorption edge show an atomic correlation at the characteristic distance for an oxygen shell. Unfortunately, it was not possible to normalize the data to obtain useful co-ordination numbers.

5. Conclusions

The mapping of the absorption profiles of the core regions of these samples has demonstrated the close correlation between the concentration of erbium

atoms and the germanium present, i.e. the erbium ions introduced via the solution doping technique [2] follow the germanium concentration profile established during the core soot deposition phase of the MCVD process.

The results demonstrate that evaporative losses affecting the germanium dopant also affect the erbium incorporated into the preform core. If the assumption that the erbium tracks the germanium profile is valid, measurements of the refractive index profile, which are dependent upon the germanium content of the glass, would also be representative of the erbium concentration.

The germanium atoms have been shown to be incorporated into the silica matrix with the first shell comprising approximately eight oxygens, and their next nearest neighbours being predominantly silicon, though the exact magnitude of evaluated coordination numbers suffer from experimental uncertainties. However, there are indications that the erbium atoms may also be correlated to the second shell about the Ge atoms, although no definitive information is accessible.

Acknowledgements

DTB would like to acknowledge financial support from Pirelli Cables Ltd, and The Physics Laboratory of the University of Kent at Canterbury. We would like to thank the Daresbury Laboratory for access to the SRS to perform these experiments.

References

1. C. K. KAO, "Optical Fibre" (Peter Peregrinus, IEEE, London, 1988).
2. J. E. TOWNSEND, S. B. POOLE and D. N. PAYNE, *Electronics Lett.* **23** (1987) 329.
3. S. J. GURMAN, R. J. NEWPORT, M. OVERSLUIZEN and E. J. TARBOX, *Phys Chem. Glasses* **33** (1992) 30.
4. SERC Daresbury Laboratory, "The SRS" (1991).
5. N. BINSTED, J. W. CAMPBELL, S. J. GURMAN and P. C. STEPHENSON, "EXCURV 90" (Daresbury Laboratory, 1991).
6. N. BINSTED, S. J. GURMANN and I. ROSS, *J. Phys. C., Solid State Phys.* **17** (1984) 143.
7. *Idem, ibid.* **19** (1986) 1845.
8. S. J. GURMAN, *ibid.* **21** (1988) 3699.
9. D. W. OBLAS, T. WEI, W. J. MINISCALCO and B. T. HALL, *Mater. Res. Soc. Symp. Proc.* **172** (1990) 315.
10. R. W. JOYNER, K. J. MARTIN and P. MEEHAN, *J. Phys. C., Solid State Phys.* **22** (1987) 4005.
11. M. A. MARCUS and A. POLMAN, *J Non-Cryst. Solids* **136** (1991) 260.

Received 10 June
and accepted 13 October 1994